Astron. Astrophys. 308, L5–L8 (1996)

ASTRONOMY AND ASTROPHYSICS

Letter to the Editor

Tentative detection of a cosmic far-infrared background with COBE

J.-L. Puget[1], A. Abergel[1], J.-P. Bernard[1], F. Boulanger[1], W.B. Burton[2], F.-X. Désert[1], and D. Hartmann[2,3]

[1] Institut d'Astrophysique Spatiale, Bât. 121, Université Paris XI, F-91405 Orsay Cedex France (puget@ias.fr)
[2] Sterrewacht Leiden, Postbox 9503, 2300 RA Leiden, The Netherlands
[3] Harvard-Smithsonian Center for Astrophysics, 60 Garden St., Cambridge, MA 02138, USA

Received 4 August 1995 / Accepted 12 December 1995

Abstract.

We have searched for an extragalactic far infrared background in the whole sky survey of the Cosmic Background Explorer (COBE) Satellite, using data from the Far Infrared Absolute Spectrometer (FIRAS) instrument. We model and remove the interplanetary and interstellar dust components for all wavelengths above 140 microns and below a few millimetres. The new Leiden/Dwingeloo HI survey is used for the interstellar cirrus component. A component associated with the HII medium is also removed. It is found that the residues of the subtraction method have a significant positive value at all wavelengths. This emission is isotropic and clearly shows an excess in the submillimeter over the HI associated dust emission spectrum that cannot be explained by known or suspected solar or galactic components. We therefore suggest that it could be the cosmic far infrared background due to early galaxies that has long been predicted. Its rather large intensity can be represented by $\nu B_\nu \simeq 3.4 \times 10^{-9} (\lambda/400\,\mu\mathrm{m})^{-3}\,\mathrm{W\,m^{-2}\,sr^{-1}}$ in the 400-1000 μm range and levelling off at shorter wavelengths. It implies that a large fraction of the radiation of early galaxies has been converted in the far IR. The spectrum seems to indicate the presence of sources at large redshifts (typically $z \approx 3 - 10$).

Key words: cosmology:observations ;diffuse radiation – galaxy:formation

1. Introduction

A cosmic background radiation has long been predicted (Partridge & Peebles 1967) to exist that would trace the initial (or most important) phase of galaxy formation. The abundances of most elements observed in galaxies cannot be explained in the standard Big Bang scenario and an initial enrichment in heavy elements in galaxies must necessarily correspond to an emission of light that should be detectable. Starlight emission should then be observable in the visible and near infrared except in the case of an early presence of dust in the young galaxies. Indeed, Low and Tucker (1968), Setti & Woltjer (1970), Kaufman (1976), Stecker, Puget & Fazio (1977), and Sunyaev, Tinsley, & Meier (1978) have shown that an important Cosmic Far Infrared Background Radiation (CFIBR) could come from starlight reprocessed by dust in the host galaxies. This last hypothesis was prompted by the discovery of the first infrared galaxies. Since that time, the Infrared Astronomical Satellite (IRAS) has shown that starburst galaxies can radiate a very large fraction of their energy in the far IR (Soifer, Houck & Neugebauer 1987). Many models have since been developed to predict the CFIBR (*e.g.* Beichman & Helou 1991, Désert & Puget 1990, Treyer & Silk 1993, Franceschini *et al.* 1994). Measuring this background could help in constraining the total energy involved in the galaxies and dating the galaxy formation. In the following we address, with the help of COBE data, the observability of this CIBR in the far infrared only.

So far, the CFIBR has not been evidenced owing to the strong foregrounds with spatially varying spectra and intensities, which have to be removed first. Away from the galactic plane, the main foreground emissions represent from a thousand down to a few times the expected CFIBR at wavelengths from 10 to 500 μm. Upper limits on the CFIBR have been reported; the most recent ones are given by Boulanger and Pérault 1988, Kawada *et al.* 1994, Dwek and Slavin 1994 and De Jager *et al.* 1994. Results from COBE have so far given upper limits only: using the Diffuse Infrared Background Explorer (DIRBE) data, Hauser (1995) derived these limits from 1 to 240 μm and Mather *et al.* (1994) gave the constraints on the extragalactic background in the submillimetre domain from the FIRAS measurements. Lower limits on the CFIBR have been obtained from the deepest IRAS galaxy counts at 60 μm (*e.g.* Hacking & Soifer 1991).

Here we adopt a straightforward strategy to search for the predicted CFIBR. All the foregrounds are modeled and removed using independent data sets in addition to the FIRAS data. These are the interplanetary (IP) dust emission peaking around 12–25 μm, the interstellar (IS) dust emission peaking around 150 μm, and in addition to these foregrounds the CMBR peaking around 1 mm. The main difficulty arises from the fact that Galactic emission can mimic the CFIBR. Hence it is difficult to be sure at DIRBE wavelengths ($\lambda \leq 240\,\mu$m) that one is really in front of an extragalactic background and not an untraced galactic component. On the other hand, the CFIBR is likely to have a submillimetre component. Indeed, most models of galaxy formation (*e.g.* Franceschini *et al.* 1994) predict that

Send offprint requests to: J.-L. Puget

the ratio of CFIBR to the foregrounds increases with wavelength. The best cosmological spectral window is therefore in the submillimetre domain between 200 and 800 μm. Hence, FIRAS is adapted to the search of the CFIBR. Next section describes the data sets which are used. Then the decomposition strategy of the sky brigthness is applied. The resulting residual component is then analysed. Finally, discussion and possible explanations are given. A separate paper (Boulanger *et al.* 1996) discusses in much more detail the far IR emission from the different IS diffuse components (see also Boulanger *et al.* 1995).

2. Data description

In order to model the different FIR components of the sky emission spectrum, we basically use their different spatial distribution and assume a constant spectral behavior. The IP dust is traced by the 25 μm DIRBE channel. The best tracer of most of the diffuse interstellar medium at high galactic latitude is the 21 cm line. The fully calibrated, all-sky COBE data sets which are described in the following, were released in the public domain in September 1994. The successful COBE cryogenic life spanned the range from November 1989 to September 1990 (*e.g.* Boggess *et al.* 1992).

DIRBE on board the COBE is a photometer that provides absolute sky brightness measurements in 10 wavelength bands from 1 to 240 μm (see Silverberg *et al.* 1993). We degraded DIRBE resolution of 0.7° to FIRAS resolution in order to map the IP dust emission. We used the 90° solar elongation maps as the closest in solar elongation from FIRAS data.

FIRAS on board the COBE is a Michelson interferometer with a horn with very low side lobes that gives a 7° beam on the sky. The full calibration is detailed by Fixsen *et al.* (1994). We use the data taken in the so-called RHSS and LLSS modes, covering the 105 to 5000 μm range and 500-5000 μm range respectively. For each pixel on the sky (at 2.6° sampling), a spectrum at constant $\Delta\nu$ resolution of 0.8 cm^{-1} is obtained. The LLSS data have better signal to noise ratio than the RHSS at wavelengths above 500 μm. The RHSS data at wavelengths smaller than 170 μm were too noisy to give useful information.

The Leiden–Dwingeloo HI survey (Hartmann & Burton 1995) was obtained with a 36' beam sampled every 30' and a velocity resolution of 1 km/s, north of -30° declination. Corrections for stray light were thoroughly done (Hartmann 1994).

3. Foreground removal

DIRBE 25 and 100 μm ecliptic latitude profiles are first derived, by taking the minimum values for all ecliptic longitudes. The average brightness ratio $B_\nu(100)/B_\nu(25)$ is found to be 0.167. Reach *et al.* (1995) found with FIRAS data that the submillimeter spectrum of zodiacal light is quite steep with $B_\nu \propto \nu^3$. Thus we model the zodiacal FIRAS spectrum for each line of sight by using the 25 μm DIRBE ecliptic latitude profile scaled by $0.167\,(\lambda/100\,\mu\mathrm{m})^{-3}$.

We directly model the CMBR spectrum and the dipole component found in the FIRAS data by Mather *et al.* (1994). Thereafter, the CMBR and Zodiacal light are both subtracted from the raw FIRAS spectrum at each pixel.

The submillimetre emission is dominated by IS dust mostly associated with atomic gas at high latitude. As shown by Boulanger *et al.* (1996), the FIRAS spectrum correlates quite well with the HI tracer spectrally integrated between -100 and 100 km/s and degraded to the FIRAS resolution. They interpret the pixels which have an infrared excess over the main correlation as some molecular clouds or clouds with a local heating source. Thereafter we restrict the study to high galactic latitudes ($|b| \geq 20°$) and to low column density lines of sight ($N_{\mathrm{HI}} \leq 4.5 \times 10^{20}\,\mathrm{H\,cm^{-2}}$, using 1 $\mathrm{K\,km\,s^{-1}} = 1.82 \times 10^{18}\,\mathrm{H\,cm^{-2}}$), where there is little molecular gas, and without infrared excess, in order to minimise the impact of galactic emission. Boulanger *et al.* (1996) find that the HI correlated submillimetre emission of IS dust closely matches a modified blackbody curve at a temperature of 17.5 K with a ν^2 emissivity law. This template is scaled to the HI column density and subtracted from the FIRAS spectrum at each point. The residual spectrum is shown as the thick line in Fig 1. It is likely that it still contains some residual galactic emission associated with the ionised gas (*e.g.* at high altitudes). Boulanger *et al.* (1996) have attempted to estimate its contribution by looking at galactic gradients of this residual emission. Based on their best estimate, we subtract the infrared emission equivalent to a column density of $0.4 \times 10^{20}\,\mathrm{H\,cm^{-2}}$.

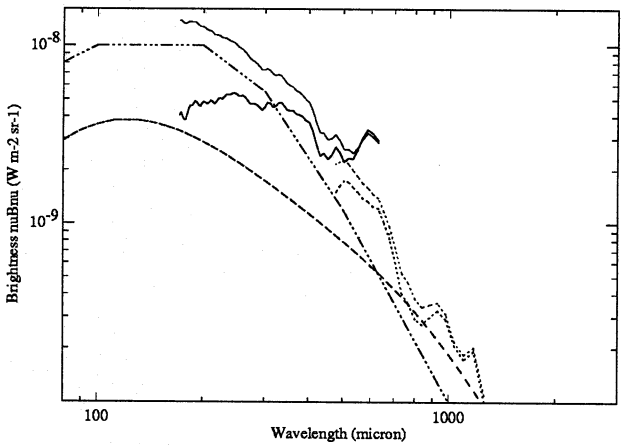

Fig. 1. Residual FIRAS spectrum after CMB, zodiacal and cirrus emission removal, averaged over low cirrus emission regions. The solid and dotted curves come from the high (RHSS) and low frequency (LLSS) FIRAS channels respectively. A constant $\Delta\nu/\nu = 0.05$ smoothing was applied. For the lower thick curve, the IR emission associated with H^+ emission is removed (see text). The dashed and dot-dot-dot-dash curve are models by Maffei *et al.* (1996) and Franceschini *et al.* (1994, see Sec. 4) respectively.

4. Properties of the residual component

4.1. Spectral properties

The thick line in Fig. 1 represents the residual spectrum after removal of all the foregrounds discussed above. A preliminary report of this residual component (for the RHSS high frequency data only) was given by Désert *et al.* 1995. The shallow peak emission happens at around $\lambda \simeq 250$ μm and roughly follows a power-law $\nu B_\nu \simeq 3.4 \times 10^{-9} (\lambda/400\,\mu\mathrm{m})^{-3}\,\mathrm{W\,m^{-2}\,sr^{-1}}$ in the 400-1000 μm range. It cannot be accounted by any scaling of the HI template emission spectrum and no single blackbody curve can model this component. Systematic offsets in FIRAS cannot account for this residual component at the level of $2 \times 10^{-10}\,\mathrm{W\,m^{-2}\,sr^{-1}}$ at wavelengths longer than

500 μm (Mather *et al.* 1994, Hauser *et al.* 1995, FIRAS Expl. Supp. 1995). Similarly, residual errors in the stray light corrections on HI data would tend to underestimate the residual component that is evidenced here. Also, a bias in the amount of infrared emitting gas using the HI tracer cannot produce such a residual (Boulanger *et al.* (1996). Let us notice that this residual spectrum contribute to one third of the sky brightness around 500 μm in the darkest galactic patches, a non negligible fraction. At 500 μm, our findings are slightly above the upper limits to any residue as given by Hauser (1995) from the FIRAS upper limits on the CMBR distortions (Mather *et al.* 1994). In fact, these last authors used the DIRBE 240 μm band to subtract the "galactic component" in their signal. This procedure clearly underestimates any possible residual component which is spectrally close to (but different from) the all-sky galactic dust emission spectrum, as Mather *et al.* already cautioned. The main uncertainty in the thick line spectrum in Fig. 1 is typically 2×10^{-9} W m^{-2} sr^{-1} coming from H^+ removal at wavelengths smaller than 300 μm. It is lower at longer wavelengths ($\simeq 2 \times 10^{-10}$ W m^{-2} sr^{-1} around 800 μm) coming from detector noise. Below 170 μm the systematic errors (including ZL subtraction uncertainties) become comparable to the residual flux. Notice that the two datasets (solid and dotted lines) give consistent results. The low frequency dataset is of much better signal to noise ratio in the common wavelength range.

4.2. Spatial distribution

Fig. 2 shows the histogram of the residual specific brightness integrated between 400 and 600 μm and expressed at an effective wavelength of 500 μm. The mean brightness is 2.4×10^{-9} W m^{-2} sr^{-1} and clearly different from the zero level. The uncertainty on this value is certainly dominated by systematic effects in the foreground subtraction method. The histogram has a very small asymmetry. Its FWHM of $4 - 6 \times 10^{-9}$ W m^{-2} sr^{-1} (for the 2 channels respectively) is dominated by measurement noise, indicating that this component is essentially isotropic. The statistical error on the determination of the mean is of the order of 1.5 10^{-10} W m^{-2} sr^{-1}, smaller than the systematics effect discussed above. The zodiacal emission intensity that was removed is of the order of 10% of the residual component. Even assuming a conservative 50% uncertainty in zodiacal light modeling, the resulting uncertainty is less than 5%. This is confirmed by the absence of longitude and latitude dependency in ecliptic coordinates plots. Therefore we focus now on any possible galactic anisotropy. The residual is displayed averaged in galactic latitude bins in Fig. 3a and longitude bins in Fig. 3b. There is no systematic dependence of the residual with either galactic latitude or longitude. Similar conclusions are reached when the residual is integrated between 600 and 1000 μm.

5. Discussion

We discuss here the possible origins for the isotropic component found in the previous section. The isotropic component, if produced by thermal emission, must fulfill the following conditions: the emission in the 400 μm to 1 mm has a modified Rayleigh-Jeans dependence whereas it is rather flat between 200 and 400 μm. For any type of thermal emission this implies a typical set of temperatures and emissivities for the emitting sources (assuming black body spectra) with particles at 20 and 12 K with an emissivity of 3×10^{-6} and 5 K with an emissivity

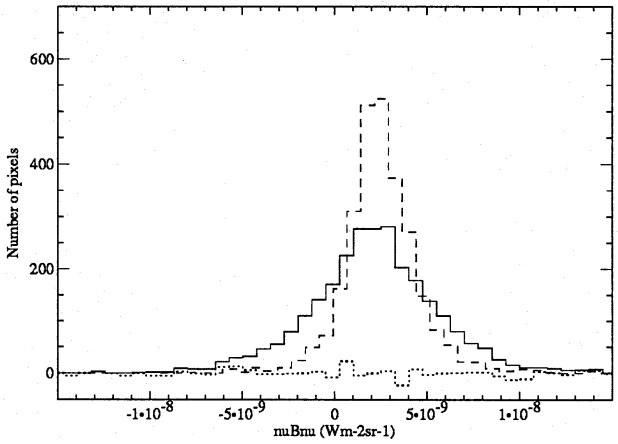

Fig. 2. Histogram of the residual brightness at 500 μm after smoothing of about 7 ° has been applied to the original data. The solid (resp. dashed) line comes from the high (resp. low) frequency channel. The dotted curve is obtained by subtracting a symmetric version of the dashed histogram around its mean value.

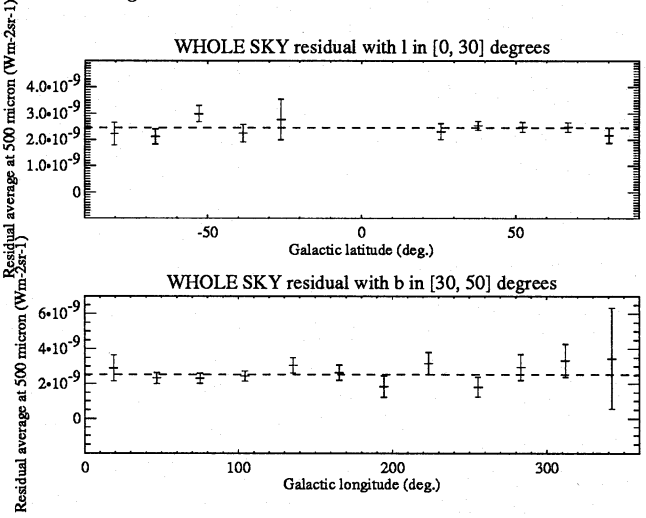

Fig. 3. Residual brightness dependence with galactic latitude and longitude at 500 μm (for the low frequency channel). The error bars are statistical errors of the mean in each latitude or longitude bins. The dashed horizontal line is the grand average value.

of 3×10^{-5} implying that most of the material should be very cold with temperatures extending down to values close to the temperature of the CMB.

5.1. Interplanetary emission origin

The residual component cannot be created by the uncertainties in the removal of the observed zodiacal cloud. The overall isotropy rules out an origin in the Kuiper belt or the inner Oort cloud. It could only be due to an emission coming from the outer solar system: the Oort cloud. The Oort cloud which is the reservoir of long period comets has a typical radius of $R_{cl} = 50000$ AU and contains $N_c = 10^{11}$ to 10^{12} comets (Weissman 1985); the temperature of massive absorbing objects in the outer solar system is controlled by the galactic and CMB radiation field and is around 4K. With the parameters

above, the emissivity associated with the Oort cloud is given by $\tau = 1.3 \times 10^{-15}(R_{comet}/1\,km)^2$. This value is very small compared to the needed value of 3×10^{-5}. Even splitting the total mass of comets in 1 cm grains would not account for the observed flux. Furthermore, grains of these size would be swept out of the solar system gravitational potential well by the interaction with the ISM.

5.2. Galactic emission origin

A temperature variation on different lines of sight cannot generate the residual component as it is colder than expected from a differential blackbody around 17 K. Reach *et al.* (1995) find from analyzing FIRAS data alone that some cold dust (7 K) must be present in the ISM even at high galactic latitudes and is correlated with the warmer (17 K) component. Boulanger *et al.* (1996) have shown that this cold component, if it exists, does not belong to the disk.

To get a galactic emission with a very weak latitude and longitude dependence, this emission must be generated in a spherical shell with an inner radius R larger than 60 kpc to keep the anisotropy in longitude smaller than 20% at a latitude of 45 °. At this distance, most of the dust would be very cold (typically below 5 K in the intergalactic radiation field) and would produce a spectrum narrower than the one shown in Fig. 1. In addition, such a halo would correspond to a bright source with total flux $\simeq 1000Jy(D/1Mpc)^{-2}$ at 300 μm, which would have been easily detected toward external galaxies, if such haloes were common. A galactic origin seems thus to be ruled out.

5.3. Extragalactic origin

We can easily rule out any uncertainty in the temperature of the CMBR removed as a source of this isotropic background because the residual would exhibit an exponential fall–off at wavelengths smaller than 1 mm. Similarly a secondary distortion of the CMB due to Compton interaction with some hot gas (the Sunyaev–Zeldovich effect) would also present an exponential fall–off. Other more exotic models have been suggested for such a background, for example decay of massive particles (Bond, Carr and Hogan 1986).

As discussed in the introduction, if the observed isotropic component is due to early galaxies, which is the least contrived hypothesis, some important consequences for galaxy formation can be derived. The amount of energy in the background is rather large because it exceeds the predictions based on minimal extrapolations of the starburst galaxies seen in the IRAS deep surveys by about a factor of 3. Thus it requires other sources like spheroidal systems radiating mostly in the far infrared during their early evolution as suggested by the model of Mazzei *et al.* (1994). Elbaz *et al.* 1995 have also postulated a high formation rate of massive stars at the early stages of evolution of elliptical galaxies to account for the enrichment of the cluster gas in heavy elements. The model of Franceschini *et al.* (1994) built on this hypothesis accounts rather well for the background. If elliptical galaxies form as IR dominated objects, as suggested by the Mazzei *et al.* 1994 model and have spectra similar to the ultra luminous galaxies (peaking at around 60 μm) some of them must form at redshifts as large as 10. If the first objects to form are lower mass ones as expected in many current models of structure formation the peak of emission would be at longer wavelength (150 μm) requiring a redshift of formation of the earliest objects which could be around 3.

Acknowledgements. Part of this work was supported by a CNES-INSU grant. The COBE datasets were developed by the NASA Goddard Space Flight Center under the guidance of the COBE Science Working Group and were provided by the NSSDC. The Dwingeloo 25-m telescope is operated by the Netherlands Foundation for Research in Astronomy with support from the Netherlands Organisation for Scientific Research (NWO).

References

Beichman, C. & Helou, G., 1991, ApJL, 370, L1
Boggess, N. W. *et al.* 1992, ApJ, 397, 420
Boulanger, F., Pérault, M., 1988, ApJ, 330, 964
Boulanger, F. *et al.* 1996, AA, submitted
Boulanger, F. *et al.* 1995, in "Unveiling the Cosmic Infrared Background" ed. E. Dwek, (AIP Conf. Proc.)
Bond, J. R. *et al.* 1986, ApJ, 306, 428
Désert, F.–X., & Puget, J.–L., 1990, in Proceed. of IAU Symp. 139, eds S. Bowyer & Ch. Leinert, (Kluwer: Dordrecht), p. 381
Désert, F.–X. *et al.* 1995, "Unveiling the Cosmic Infrared Background" ed. E. Dwek, (AIP Conf. Proc.)
Dwek, E., & Slavin, J., 1994, ApJ, 436, 696
De Jager, O. C., *et al.* 1994, Nature, 369, 294
Elbaz, D. *et al.* 1995, AA, 303, 345
Fixsen, D. J. *et al.* 1994, ApJ, 420, 457
Franceschini, A. *et al.* 1994, ApJ, 427, 140
Hacking, P. B., & Soifer, B. T., 1991, ApJL, 367, L49
Hartmann, D., 1994, Ph. D. Thesis, University in Leiden.
Hartmann, D., Burton, W.B. 1995, An Atlas of Galactic Neutral Hydrogen Emission, Cambridge University Press, under contract.
Hauser, M. G., 1995, in Proceed. of IAU Symp. 168, The Hague, Aug 94
Hauser, M. G. *et al.* 1995, "Unveiling the Cosmic Infrared Background" ed. E. Dwek, (AIP Conf. Proc.)
Kaufman, M., 1976, Ap and Sp Sc, 40, 369
Kawada, M. *et al.* 1994, ApJL, 425, L89
Low, F. J., & Tucker, W. H., 1968, Phys. Rev. Lett., 21, 1538
Mather, J. C. *et al.* 1994, ApJ, 420, 439
Maffei, B. *et al.* 1996, in preparation
Mazzei, P. *et al.* 1994, ApJ, 422, 81
Partridge, R. B., & Peebles, P. J. E., 1967, ApJ, 148, 377
Reach, W. T. *et al.* 1995, ApJ, in press
Silverberg, R. F. *et al.* 1993, in SPIE Conference Proc 2019 on *Infrared Spaceborne Remote Sensing*, San Diego, July 93.
Soifer, B. T. *et al.* 1987, ARA&A 25, 187
Stecker, F. W. *et al.* 1977, ApJL, 214, L51
Sunyaev, R. A. *et al.* 1978, Comments Ap Space Sci., 7, 183
Treyer, M.–A., & Silk, J., 1993, ApJL, 408, L1
Weissman P.R., 1985, Protostars and Planets II, B.C. Black & M.S. Matthews Eds, 895.
Setti G., & Woltjer L, 1970, Nature, Lond. 227, 586

This article was processed by the author using Springer-Verlag LaTeX A&A style file 1990.